CrossMark

Palladium supported on phosphorus–nitrogen dual-doped carbon nanoparticles as cathode for hydrogen evolution in PEM water electrolyser

S. Shiva Kumar [1,2] · S. U. B. Ramakrishna [1,3] · K. Naga Mahesh [3] · B. Rama Devi [2] · V. Himabindu [1]

Abstract

Phosphorus–nitrogen dual-doped carbon nanoparticles (PN-CNPs) have been successfully synthesised using chemical vapour deposition (CVD), in the presence of triphenylphosphine and acetonitrile. PN-CNPs are used as carbon support for Pd and employed as electrocatalyst in hydrogen evolution reactions. The prepared Pd/PN-CNPs electrocatalyst was subjected to morphological and electrochemical studies carried out using FE-SEM, EDS, ICP, XRD, CV, and LSV techniques. The membrane electrode assemblies (MEAs) were prepared and tested in 25 cm^2 area PEM cell setup and the test results obtained are promising as the cell voltage is 1.9 V at 1000 mA cm^{-2} at 80 °C. Furthermore, the cell setup was operated continuously for 500 h and has shown stable performance without any hindrance in electrochemical activity.

Introduction

Hydrogen is a promising fuel, can be produced from various sustainable and renewable energy sources [1–3]. Electrolysis of water using PEM technology is compact and one of the most efficient, environmentally friendly, and sustainable methods for high pure hydrogen production [4–6]. In PEM water electrolysis, precious metals are used as the electrocatalysts such as platinum (Pt) or palladium (Pd) at the cathode for hydrogen evolution reaction (HER) and IrO$_2$ or RuO$_2$ at the anode for oxygen evolution reaction (OER) [7, 8]. However, one of the main

✉ V. Himabindu
    drvhimabindu@jntuh.ac.in

1   Center for Alternative Energy Options, Institute of Science and Technology, Jawaharlal Nehru Technological University Hyderabad, Kukatpally, Hyderabad, Telangana 500085, India

2   Department of Chemistry, College of Engineering Hyderabad, Jawaharlal Nehru Technological University Hyderabad, Hyderabad, Telangana 500 085, India

3   Centre for Advanced Energy Studies, Koneru Lakshmaiah Education Foundation, Green Fields, Vaddeswaram, Guntur, Andhra Pradesh 522 502, India

challenges in PEM electrolysis is to reduce the noble metal usage and to maintain the high cell efficiencies. This can be achieved by developing noble metals supported by different carbons with large surface area low-cost electronic carriers [7], typically, carbon nanomaterials, carbon blacks used as electronic carriers due to its high electronic conductivity, corrosion resistance, surface properties, and low cost [9]. During the last decade, various carbons were studied, like carbon black, CNTs, graphene, fullerenes, etc. [10–12]. Recently, heteroatom-doped (N, P, B and S) carbon nanomaterials have gained interest in industry and academia due to the long-term operational stability and relatively low cost [5, 13, 14]. The introduction of heteroatoms within the lattice of carbon matrix creates structural defects due to difference in electronegativity and atomic size. The defects in carbon favour improvement of charge exchange characteristics by anisotropy. The heteroatom (P, N) doping drastically changes carbon framework, improves the charge density and hydrophilicity, and decreases charge transfer resistance [15, 16].

Nitrogen-doped carbon nanomaterials exhibit excellent electrochemical performance towards the HER and OER, can be attributed to incorporation to the heteroatoms in the carbon matrix, which break the catalyst's electro neutrality to create electrochemically active sites, and therefore favour the molecular adsorption and reduction of oxygen [17–19].

Recently, heteroatoms other than N have been studied, including phosphorus [18, 20], sulphur [21], and boron [22]; these materials have also shown enhanced electrocatalytic activity towards the oxygen reduction reaction (ORR), but the electrochemical performance is still lower than conventional Pt/C catalysts. To address the challenges, several researchers have reported that doping carbon materials with two or three heteroatoms can further improve their electrochemical performance. For example, Choi et al. studied that P, N dual-doped carbon materials show higher catalytic activity than the single N-doped carbon in ORR, indicating that the supplementary P doping could significantly improve the electrocatalytic activity [23, 24]. Similar contribution to the enhancement of specific capacitance by P, N dual doping and single P doping for carbon materials is studied in supercapacitors [25, 26]. Although the performance of P- and N-doped carbon materials for the applications in fuel cells has been extensively investigated, the P and N are in the same family and higher electron-donating ability and exhibits stronger n-type behaviour [27, 28].

Nitrogen (N) incorporation into the carbon materials enhances electrical conductivity and adsorption properties. Phosphorus (P) doping into CNPs resulted in a negative charge density in the carbon atoms because of the lower electronegativity of phosphorus (2.19) than that of C (2.55) and therefore a high activity towards the HER [29]. Furthermore, the structural modification of carbon by phosphorus doping will be more effective, because phosphorus has a much larger covalent radius (107 ± 3 pm) than carbon (73 ± 1 pm). This is important in the enhancement of the HER activity of carbon. Therefore, while doping the P and N onto the CNPs significantly enhances the electrochemical performance. The application of P–N dual-doped CNPs towards HER in PEM water electrolysis has less studied.

In the present study, phosphorous–nitrogen dual-doped CNPs have been successfully synthesised using spray-pyrolysis technique in chemical vapour deposition (CVD) method and used as a support material for Pd. The synthesised Pd/PN-CNPs have been used as cathode and RuO_2 as anode in the fabrication of MEA. These prepared MEAs were tested and evaluated in in-house fabricated single-cell PEM water electrolyser along with the corresponding yields of hydrogen.

Materials and methods

Materials

Palladium (II) chloride ($PdCl_2$), triphenylphosphine (TPP), and ruthenium (IV) oxide (RuO_2) were purchased from Sigma Aldrich, USA. Nafion® membrane was procured from DuPont, USA. Acetonitrile (reagent grade) is purchased from Merck and Ferrocene ($Fe(C_5H_5)_2$) is purchased from SRL chemicals, India.

Synthesis of phosphorus–nitrogen dual-doped carbon nanoparticles (PN-CNPs)

PN-CNPs have been synthesised by mixture of ferrocene, triphenylphosphine (TPP), and acetonitrile as precursors in chemical vapour deposition (CVD) using spray-pyrolysis technique. In this technique, 1-g ferrocene and 1-g triphenylphosphine dissolved in 100 ml of acetonitrile (CH_3CN) and the solution mixture was pyrolyzed inside the quartz tube of CVD reactor at temperature 850 °C along with argon (99.999%) gas flow at 100 sccm. After 30 min, the furnace was cooled to room temperature under the argon atmosphere. The resultant PN-CNPs were collected and purified by treating with 1:3 nitrating mixture (nitric acid and sulphuric acid) to remove amorphous carbons and residual iron particles.

Synthesis of Pd/PN-CNPs

Palladium supported on PN-CNPs electrocatalyst (Pd/PN-CNPs) has been synthesised by chemical reduction method [13, 29]. In this method, 0.75 g of $PdCl_2$ dissolved in 20 ml DI water, along with addition of 1.0 g of PN-CNPs followed by stirring for 1 h. The pH of resulting mixture adjusted to 8 by adding 1.0 M Na_2CO_3. Then, ethylene glycol (100 ml) was added to the resulting mixture solution; it acts as solvent and reagent. Further, formaldehyde (10 ml) was added dropwise. After that, reaction temperature was increased gradually to 80 °C and maintained for 2 h; after completion of the reduction, the resulting mixture solution colour turns to clear solution. Later, heating was switched off and resulting mixture was left overnight (12 h) for settling down of catalyst nanoparticles. The excess solution was decanted and washed with excess amounts of DI water, followed by washing with methanol and dried in vacuum oven at 80 °C for 12 h.

Characterisation of electrocatalysts

The synthesised Pd/PN-CNPs electrocatalyst surface morphology has been characterised by field emission scanning electron microscope (FE-SEM), (Hitachi S4700, Japan) and elemental analysis carried out by energy-dispersive X-ray spectroscopy (EDS). The amount of Pd loading on carbon support was determined by ICP method. The structural properties of the Pd/P-CNPs were carried out using Philips PW3050/60 X-ray generator and fitted with an X'Celerator with Cu-Kα radiation ($\lambda = 1.540598$ Å). The data collected over a 2θ range of 10–80° with a scan speed of 2 degree min^{-1}. All scans were carried out in continuous mode using the X'Celerator RTMS detector.

Electrochemical studies were carried out using Gamry Ref 600 Potentiostat/Galvanostat. Cyclic voltammetry (CV) and linear sweep voltammetry (LSV) were employed to study the electrochemical performance of prepared electrocatalysts. All experiments were performed in a conventional three electrode assembly using GC, Pt wire, and SCE as working, counter, and reference electrodes respectively and the electrolyte is 0.5 M H_2SO_4 solution.

Fabrication of MEAs

Nafion® 115 polymer membrane (DuPont, thickness 127 μm) was used to fabricate the MEAs. Prior to fabrication of MEAs, Nafion® 115 membrane was pre-treated to remove impurities of organic and inorganic by boiling at 80 °C in 3% H_2O_2 solution for 1 h followed by washing with DI water. Later, the membrane was boiled in 0.5 mol L^{-1} H_2SO_4 solution for 1 h and by washing with DI water. Finally, the membrane was again boiled in DI water for 1 h and stored in DI water [30, 45].

The MEAs were fabricated using Pd/PN-CNPs and RuO_2 electrocatalysts for HER (cathode) and OER (anode) respectively. The Pd/PN-CNPs (30 wt% Pd/PN-CNPs) were ultrasonically dispersed in a mixture of Nafion® solution (5 wt%, DuPont, USA), water, and isopropyl alcohol to form homogeneous electrocatalyst slurry. Later, the prepared electrocatalyst slurry was directly sprayed on carbon cloth with the metal loading of 0.7 mg cm^{-2} as the cathode for HER electrode. Similar preparation process was followed for OER electrode, RuO_2 as electrocatalyst on anode side with typical metal loading of 3 mg cm^{-2}. Subsequently, hot pressing the catalyst-coated carbon cloth along with Nafion® 115 membrane at 120 °C and at 60 kg cm^{-2} for 3 min to form MEA [13].

PEM cell assembly

PEM single-cell assembly with 25 cm^2 active area was designed (straight parallel flow field design) and constructed with graphite plates (thickness 12 mm), and it is used to investigate the electrolysis performance and durability of the fabricated MEA. In PEM cell assembly, the fabricated MEA was placed in between two graphite plates followed by porous titanium mesh (thickness 0.5 mm) was used as a current collector, silicon rubber gaskets (thickness 0.5 mm) were used as cell adhesives with SS end plates (thickness 12 mm) along with the pencil heaters (6 mm) than assembled by nuts and bolts with a torque 8 N m^2. Later, DI water was supplied to the cell with a flow rate of 60 ml min^{-1} using a peristaltic pump and electricity to the cell was supplied using DC regulated power supply (SABA Electronics, India, 5 V–10 A). The PEM cell is operated at various set temperatures from 30 to 80 °C for better performance. The I–V characteristics of the cell were recorded, and hydrogen yield was measured by calibrated flow meter.

Efficiency of PEM water electrolysis

During electrolysis process, the water is split into hydrogen and oxygen, the energy required for splitting of water is same as the energy released during formation of water. In thermodynamic terms, the energy required for dissociation of water into hydrogen and oxygen can be represented as Gibb's free energy (ΔG) and represented below in Eq. 1.

$$\Delta G = nFE_{rev} \tag{1}$$

where

n No. of electrons involved
F 96,500 (Faraday's constant)
E_{rev} Reversible voltage

The formula used to calculate the efficiency was given below:

$$E{rev} = \frac{\Delta G}{nF} = 1.23 \text{ V} \tag{2}$$

According to the first law of thermodynamics, energy is preserved, and the conversion efficiency calculates the yield of conversion of electricity into the chemical energy. Heat is considered as a loss of useful energy. However, in water dissolution processes, some entropy is generated. Therefore, it would be more suitable to represent as enthalpy (ΔH) instead of ΔG for a potential calculation. The change in Gibb's free enthalpy is $\Delta G = 237.22$ kJ mol^{-1} and the change of enthalpy is $\Delta H = 285.84$ kJ mol^{-1} in standard conditions [31, 32]. Therefore, the minimum voltage V_{TN} (thermo-neutral voltage) required for the reaction can be calculated as:

$$V_{TN} = \frac{\Delta H}{nF} = \frac{\Delta G}{nF} + \frac{T\Delta S}{nF} = 1.48 \text{ V} \tag{3}$$

where V_{TN} is the thermo-neutral voltage, ΔS is change in entropy change at temperature T. Typically, HHV is used to calculate the efficiency of electrolysis.

$$\eta = \frac{V_{TN}}{V_{cell}} \tag{4}$$

where V_{TN} is the thermo-neutral voltage and V_{cell} is the cell voltage. The conversion efficiency of a PEM water electrolyser cell can be calculated at any current density. While operating the lower current densities at lower voltages, the electrolyser cell efficiency becomes higher [31].
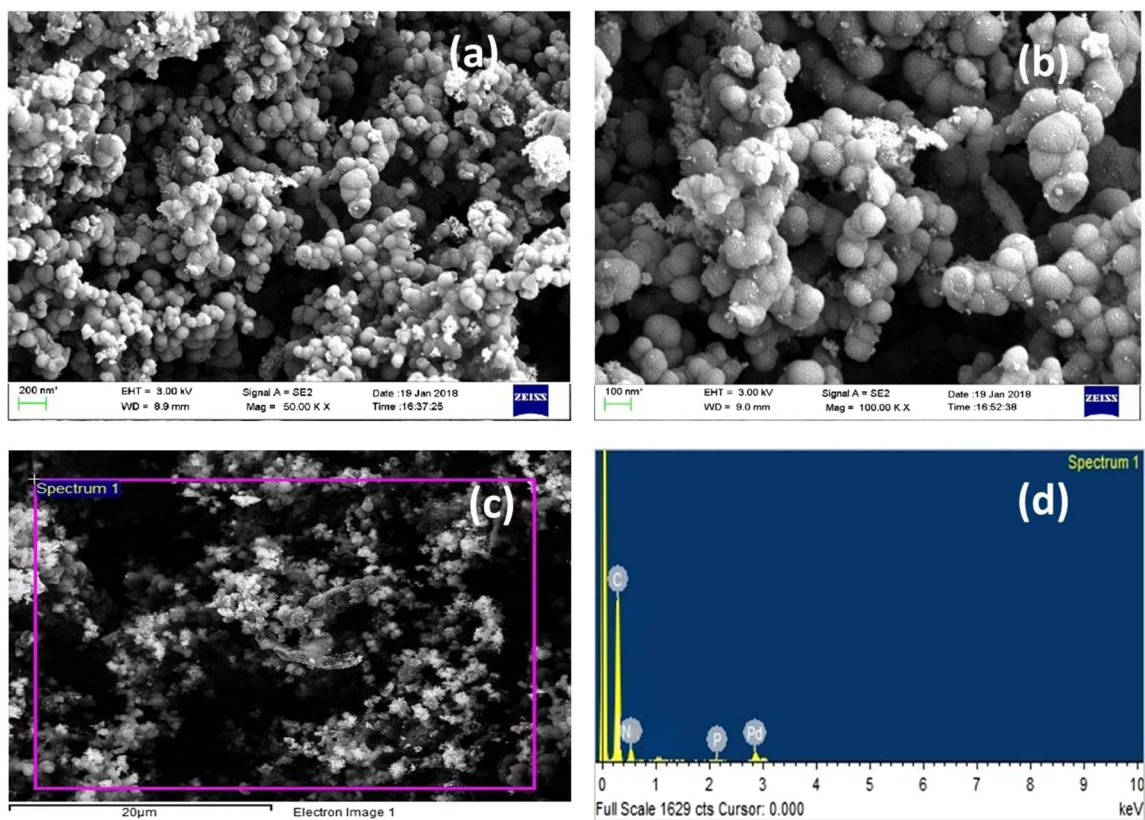
Fig. 1 **a**, **b** SEM images of Pd/PN-CNPs, **c** SEM image of Pd/PN-CNPs, **d** EDS elemental analysis spectrum of Pd/PN-CNPs

Faradaic efficiency

According to the Faraday's law, the faradaic efficiency was calculated by a ratio between the experimentally produced amounts of gas and theoretically calculated amount of gas that could be produced based on the energy input.

$$\eta_{\text{faraday}} = \frac{V_{H2}(\text{Produced})(\text{ml min}-1)}{V_{H2}(\text{Calculated})(\text{ml min}-1)} \tag{5}$$

where, the theoretically calculated amount of gas can be measured according to Faraday's second low [33]. The theoretical hydrogen yield V_{H2} (ml min^{-1}) with respect to the input

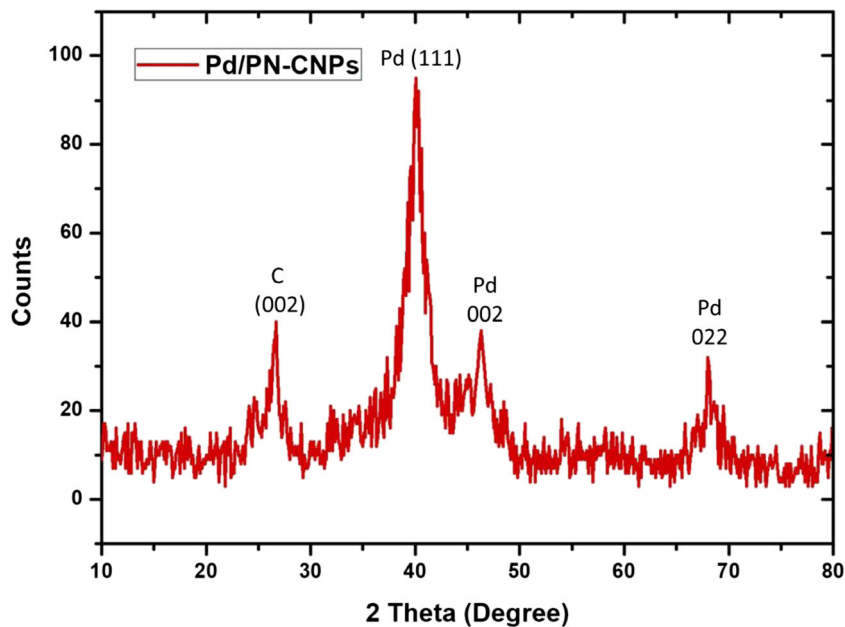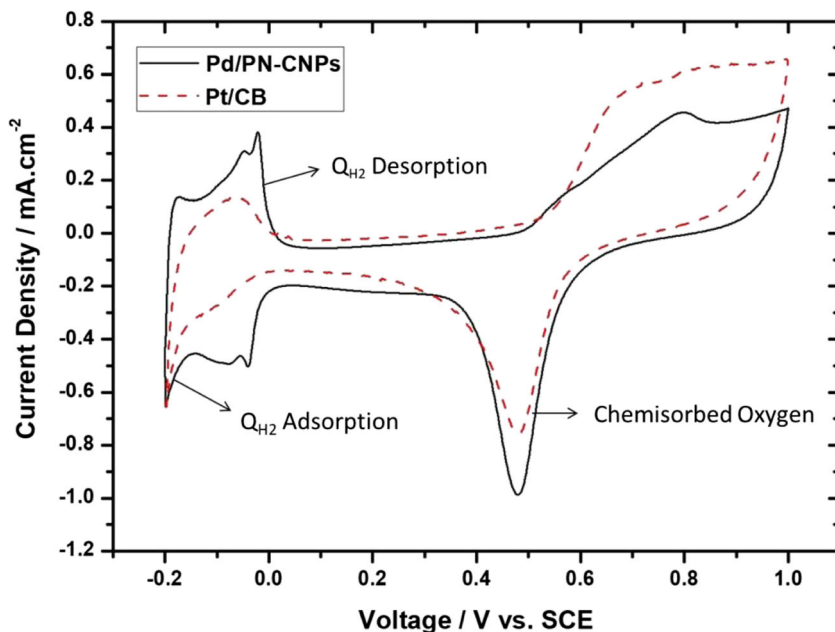**Fig. 2** X-ray diffraction patterns of Pd/PN-CNPs

Fig. 3 Cyclic voltammograms of 30 wt% Pd/PN-CNPs and 30 wt% Pt/CB in 0.5 M H$_2$SO$_4$ solutions with the scan rate of 10 mV s^{-1}
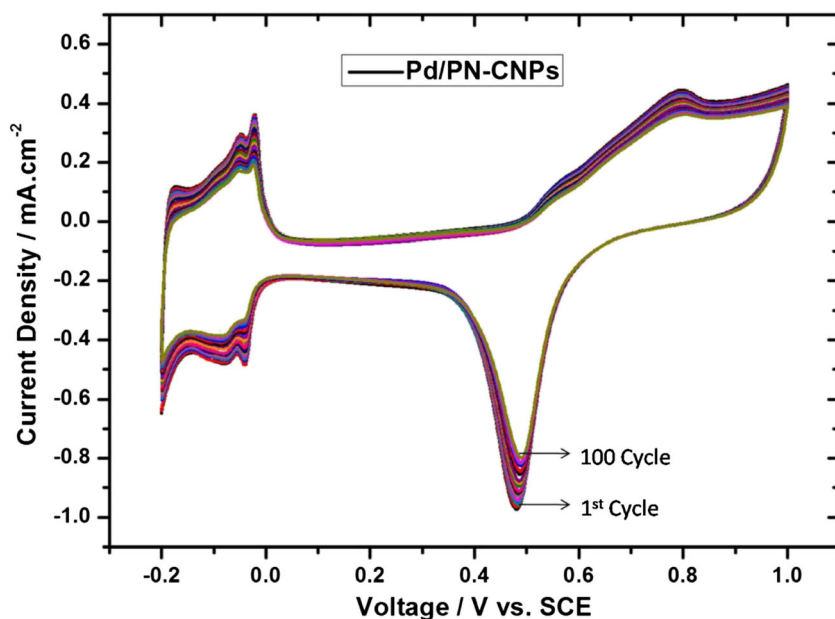

current I (A) can be calculated by Faraday's second law, which is given below

$$V_{H2} = V_M(l)\left(\frac{10^3\,\text{ml}}{1}\right)\left(\frac{t(60s)}{\text{min}}\right)\left(\frac{I\left(\frac{c}{s}\right)}{2F(C.)}\right) \quad (6)$$

where V_{H2} is the theoretical hydrogen yield (ml min^{-1}), V_M is the ideal gas expression $\left(V_M = \frac{R(273+T)}{P}\right)$, R is the ideal gas constant (0.082 l atm K^{-1} mol^{-1}), T is the temperature (°C), P is the presser (atm), t is time (s), I is the applied current (A), and F is the Faraday's constant (96,485 C mol^{-1}).

Results and discussion

Physico-chemical characterisation

Fig. 1a, b shows the FE-SEM images of Pd/PN-CNPs; the surface morphology of Pd/PN-CNPs shows spherical shape with an average diameter of 50–100 nm. A uniformly dispersed Pd nanoparticles on the surface of CNPs can be clearly seen in Fig. 1a, b. Figure 1c shows the typical SEM–EDS image of Pd/PN-CNPs and Fig. 1d shows the EDS elemental analysis of the Pd/PN-CNPs and confirms the presence of palladium (Pd), phosphorus (P), nitrogen (N), and carbon with

Fig. 4 CV stability studies of 30 wt% Pd/PN-CNPs electrocatalyst in 0.5 M H$_2$SO$_4$ solutions with the scan rate of 10 mV s^{-1}

Fig. 5 HER polarisation curves of 30 wt% Pd/PN-CNPs and 30 wt% Pt/CB in 0.5 M H_2SO_4 solutions with the scan rate of 10 mV s^{-1}
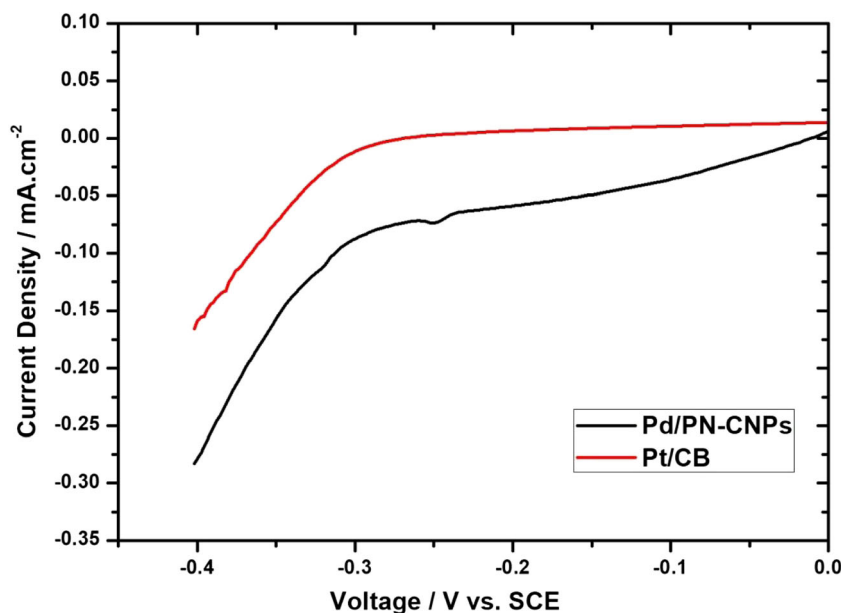
the weight percentages of 29.18%, 3.56%, 6.12%, and 61.14% respectively. Further, loading of Pd on PN-CNPs was confirmed by ICP analyser; the attained results has shown 29.92% of Pd on PN-CNPs, this is approximately equal to EDS analysis and theoretically calculated value of Pd wt%.

The synthesised Pd/PN-CNPs electrocatalyst structural properties and crystallinity have been characterised by X-ray diffraction (XRD) studies and represented in Fig. 2. The major diffraction peaks of Pd in Pd/PN-CNPs were observed at corresponding 2θ values at 40.1° {111}, 46.3° {002}, and 68.0° {022} and for carbon was observed at the 2θ values at 26.7° {002} [12, 13]. The sharp intense

peaks confirm the crystalline structure of the Pd/PN-CNPs. The average crystallite size was calculated from the major X-ray diffraction patterns of Pd {111} according to the Debye–Scherrer's equation [34] and represented in Eq. (7).

$$D = \frac{k\,\lambda}{\beta\cos\theta} \tag{7}$$

where D, the average diameter in nm; k, the Debye–Scherrer's constant (0.89); λ, wavelength of X-rays (λ = 0.154 nm); β, full width at half maximum (FWHM) of the

Fig. 6 I–V polarisation curves of 30 wt% Pd/PN-CNPs-catalysed MEA in 25 cm^2 single-cell assembly at different temperatures 30–80 °C
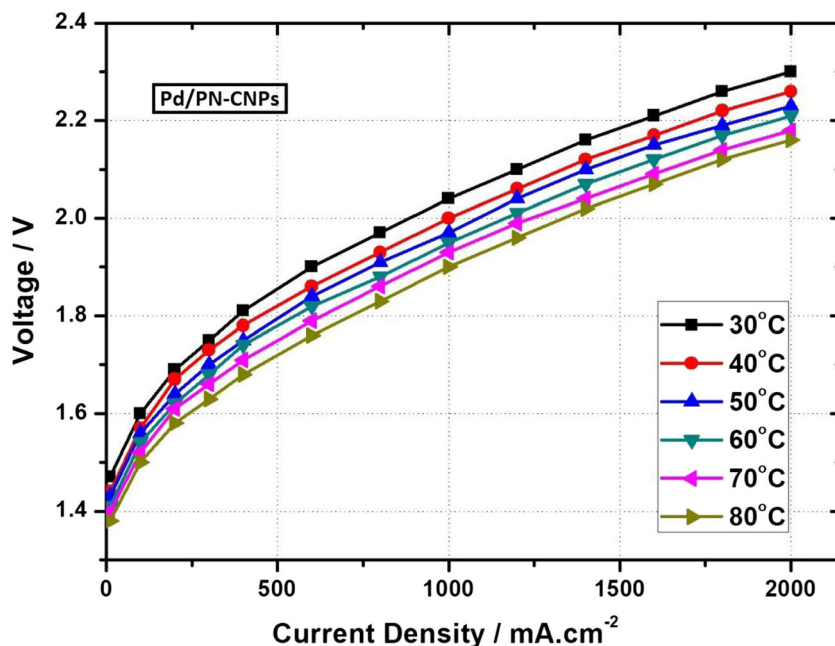
Table. 1 Hydrogen yield for 30 wt% Pd/PN-CNPs (cathode) and RuO₂ (anode)

S. No.	Hydrogen yield (L h^{-1})	Faradaic efficiency (%)	Current density mA cm^{-2}	Cell voltage (V) at 80 °C
1	6.48	96.00	500	1.72
2	12.98	96.07	1000	1.90
3	19.48	96.10	1500	2.04
4	25.98	96.11	2000	2.16

diffraction peaks; and θ, the Bragg's diffraction angle. The calculated Pd/PN-CNPs crystalline size is 4.23 nm.

Electrochemical characterisation

The synthesised Pd/PN-CNPs catalyst electrochemical performances have been studied using CV method and compared with Pt/CB, as represented in Fig. 3. CV experiments were carried out using three electrode assembly set up with GC, SCE, and Pt wire as working, reference, and counter electrodes respectively. 0.5 M H₂SO₄ solution was used as electrolyte with scan range of − 0.2 V–1.0 V. The HER occurs at the starting scan potential of − 0.2 V. During the CV experiments, the increase and decrease in current during reverse scan from − 0.2 to 0.4 V might be due to the adsorbed oxygen atoms on the electrode [35]. Both the electrodes (Pd/PN-CNPs and Pt/CB) have shown well-defined hydrogen adsorption/desorption activities. However, the Pd/PN-CNPs have shown higher hydrogen adsorption/desorption capacities at the same potential compared to Pt/CB, as show in Fig. 3. Further, the electrochemical surface areas (ECSA) of the catalysts were calculated from CV results obtained for Pd/PN-CNPs and Pt/CB. The ECSA of Pt/CB was calculated using the columbic charge associate with

hydrogen desorption adatoms (Q_H) and represented in Eq. (8).

$$ECSA = \frac{Q_H}{Q_{HO} \times M} \qquad (8)$$

where Q_{HO} is an amount of electric charge per unit area for full coverage of one mono layer of hydrogen on the surface of Pt metal particle, Q_{HO} is 0.21 mC cm^{-2}, and M is the metal fraction of the catalyst taken [7, 29, 36]. The ECSA of the Pd/PN-CNPs were calculated from the mean charge of the current peaks associated with the reduction peak of chemisorbed oxygen and the current peak of hydrogen desorption was considered. The mono layer of oxygen on Pd surface considered to be 0.41 mC cm^{-2} [37, 38, 45]. The calculated ECSA of Pd/PN-CNPs and Pt/CB are 34.75 m² gm^{-1} and 30.85 m² gm^{-1} respectively. The synthesised Pd/PN-CNPs have shown higher ECSA than Pt/CB; this phenomenon might be due to difference in crystalline size of metal particles [39]. The Pd/PN-CNPs are larger in size compared to Pt/CB when taken in the same identical concentrations; it is a common trend for the faster reduction kinetics [7].

Further, CV studies of 30 wt% Pd/PN-CNPs electrocatalyst were done for to determine the durability of electrocatalyst and represented in Fig. 4. The CV experiments were done at

Fig. 7 Cell efficiency and voltage with the function of temperature with 30 wt% Pd/PN-CNPs-catalysed MEA in 25 cm² single-cell assembly
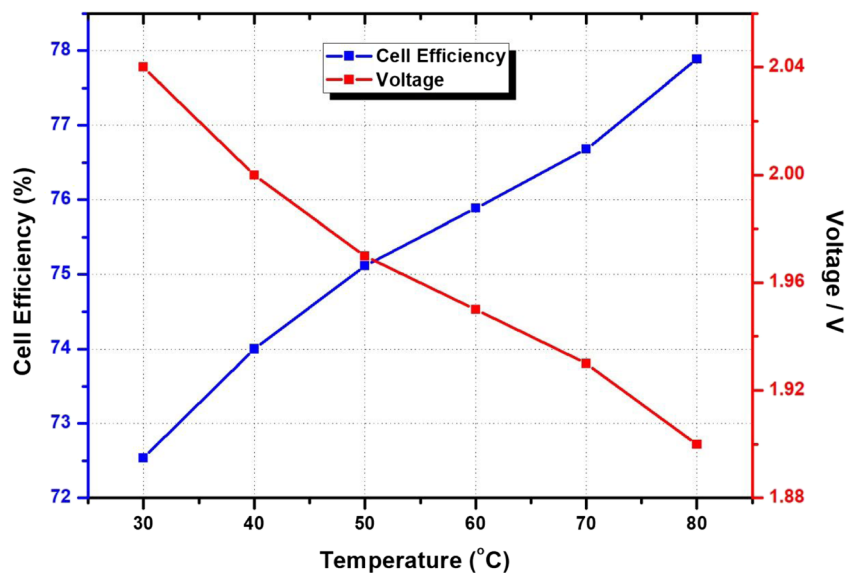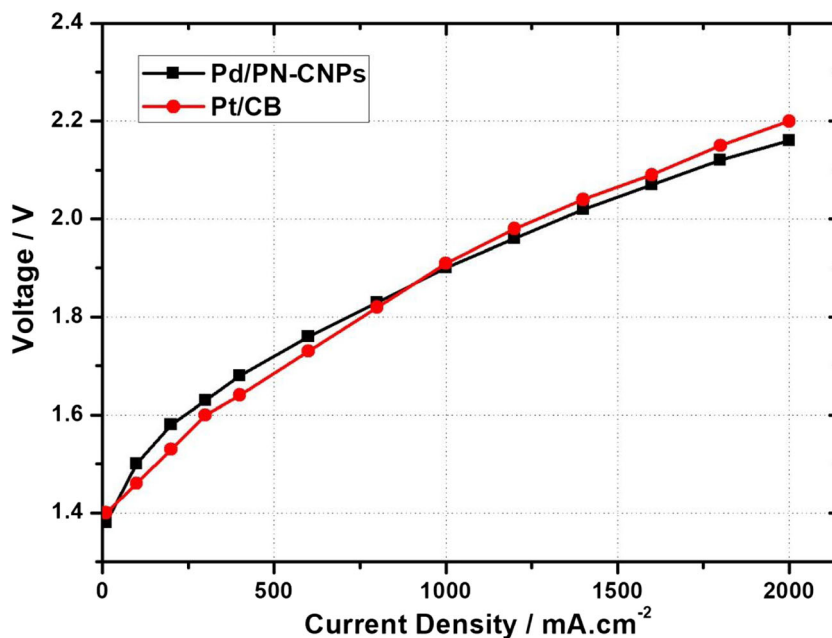
Fig. 8 I–V polarisation curves of
30 wt% Pd/PN-CNPs and 30 wt%
Pt/CB catalysed MEAs tested in
25 cm² single-cell assembly at
80 °C

10 mV s⁻¹ scan rate in 0.5 M H₂SO₄ solution. The obtained
results have shown stable electrochemical performance from 1
to 100 repetitive cycles. This might have attributed to better
structure and improved activity of the substrates [40].

LSV studies were carried out for Pd/PN-CNPs and Pt/CB to
evaluate the performance of HER. LSV experiments were done
in 0.5 M H₂SO₄ solution with the scan rate of 10 mV s⁻¹, in the
interval of 0–0.4 V corresponding to the HER region and repre-
sented in Fig. 5. The onset potential at 150 mA cm⁻² is − 0.28 V
for Pd/PN-CNPs and at 120 mA cm⁻² is − 0.3 V for Pt/CB; it
shows that the Pd/PN-CNPs have shown higher electrocatalytic

activity with increased kinetics than Pt/CB; it may be due to the
nanostructured carbon support [13, 29].

Performance of Pd/PN-CNPs in PEM cell

The fabricated Pd/PN-CNPs and Pt/CB catalysed MEAs elec-
trolysis performances were evaluated in 25 cm² single-cell
PEM water electrolyser for hydrogen production. Typically,
I–V polarisation curves were recorded with different temper-
atures (30–80 °C) along with the corresponding yields of hy-
drogen were measured and represented in Fig. 6 and Table 1.

Fig. 9 Long-term stability of
30 wt% Pd/PN-CNPs-catalysed
MEA in CC mode operated at
1000 mA cm⁻² at 80 °C
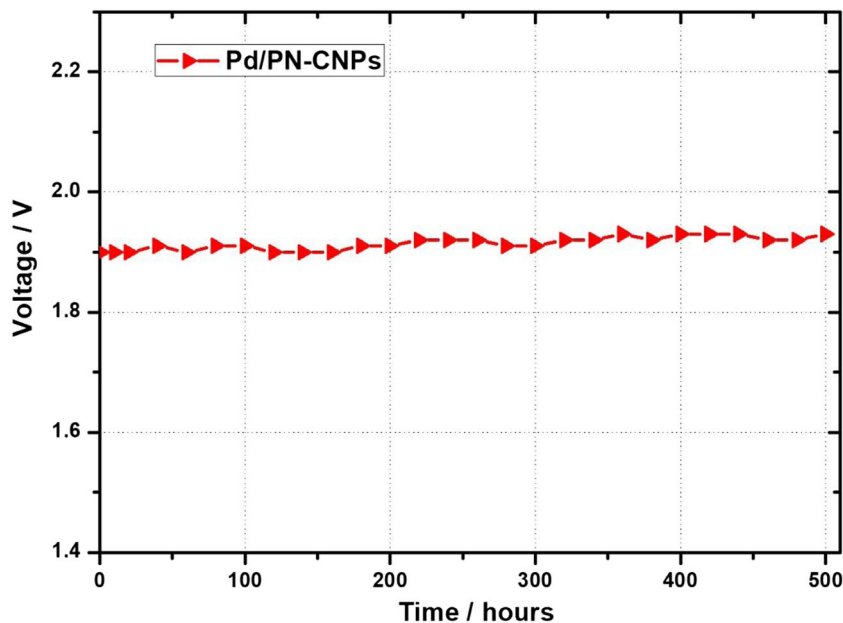
The obtained results shows that, as the temperature increased from 30 to 80 °C, the cell voltage has been reduced and the hydrogen yield has been increased significantly. This implied improved electrocatalytic activity and decrease in ohmic resistance of the cell [41–43].

However, the Pd/PN-CNPs-catalysed MEAs cell efficiency was calculated with the function of temperature and represented in Fig. 7. The calculated cell efficiency at 30 °C was obtained as 72.54% while increasing the temperature up to 80 °C; the cell efficiency also increased from 72.54 to 77.89% at 1000 mA cm^{-2} current density, due to the improvement in electrochemical activity at high temperatures [6, 29]. The faradaic efficiency of PEM water electrolyser with Pd/PN-CNPs-catalysed MEAs was calculated from the ratio between theoretical and experimental hydrogen yields. The calculated faradaic efficiency was 96% as shown in Table 1. The remaining 4% may be due to internal current losses, cell contact resistance, and gas measuring errors [39].

Further, the prepared Pd/PN-CNPs-catalysed MEAs electrolysis performances were compared with commercial Pt/CB in 25 cm^2 single cells PEM water electrolyser at 80 °C are represented in Fig. 8. The noble metal loading on MEAs for both the cases was maintained at 0.7 mg cm^{-2} at cathode and 3 mg cm^{-2} at anode. The obtained results with Pd/PN-CNPs and commercial Pt/CB were 1.9 V and 1.91 V respectively with an operating current density of 1000 mA cm^{-2} at 80 °C. The synthesised Pd/PN-CNPs has shown approximately similar performance to Pt/CB.

Further, Pd/PN-CNPs-catalysed MEAs electrolysis stability experiments were performed in 25 cm^2 single cells PEM water electrolyser at a constant current density of 1000 mA cm^{-2} at 80 °C and represented in Fig. 9. The observed cell voltage of 1.9 V at 1000 mA cm^{-2} was stable for 500-h continuous operation and the obtained results have shown better stability towards the HER in PEM water electrolyser. From the qualitative view point, the obtained results of Pd/PN-CNPs towards the HER have shown almost similar performance and stability when compared to Pt/CB owing to the synthesised Pd/PN-CNPs electrocatalyst surface area was similar to Pt/CB, well crystalline structure, and higher activity of the substrates. From the qualitative point of view, these synthesised PN-CNPs competitive with commercial carbon blacks and production method is very simple, relatively mass produced, and significantly low production cost. Consequently PN-CNPs are potentially attractive materials for HER. In the economical point of view, the Pd/PN-CNPs can be an alternative to Pt-based electrocatalysts due to low costs [9, 44].

Conclusion

Pd/PN-CNPs have been synthesised using chemical reduction method and used as HER catalyst in fabrication of MEA. The prepared Pd/PN-CNPs-catalysed MEAs performance studied

in PEM water electrolyser and their performance was compared with commercial Pt/CB. The obtained results show that the Pd/PN-CNPs-catalysed MEAs have shown similar electrochemical activity compared to Pt/CB, probably due to its nanostructured carbon support. Palladium which is less expensive compared to platinum can be an alternative to platinum for HER, HOR applications.

References

1. Nikolaidis P, Poullikkas A (2017) A comparative overview of hydrogen production processes. Renew Sust Energ Rev 67:597–611. https://doi.org/10.1016/j.rser.2016.09.044
2. Barbir F (2005) PEM electrolysis for production of hydrogen from renewable energy sources. Sol Energy 78:661–669. https://doi.org/10.1016/j.solener.2004.09.003
3. Garcıa-Valverde R, Espinosa N, Urbina A (2012) Simple PEM water electrolyser model and experimental validation. Int J Hydrog Energy 37:1927–1938. https://doi.org/10.1016/j.ijhydene.2011.09.027
4. Grigoriev SA, Porembsky VI, Fateev VN (2006) Pure hydrogen production by PEM electrolysis for hydrogen energy. Int J Hydrog Energy 31:171–175. https://doi.org/10.1016/j.ijhydene.2005.04.038
5. Grigoriev SA, Mamat MS, Dzhus KA, Walker GS, Millet P (2011) Platinum and palladium nano-particles supported by graphitic nano-fibers as catalysts for PEM water electrolysis. Int J Hydrog Energy 36:4143–4147. https://doi.org/10.1016/j.ijhydene.2010.07.013
6. Siracusano S, Baglio V, Briguglio N, Brunaccini G, Di Blasi A, Ornelas A, Trifoni E, Antonucci V, Arico AS (2012) An electrochemical study of a PEM stack for water electrolysis. Int J Hydrog Energy 37:1939–1946. https://doi.org/10.1016/j.ijhydene.2011.06.019
7. Grigoriev SA, Millet P, Fateev VN (2008) Evaluation of carbon supported Pt and Pd nanoparticles for the hydrogen evolution reaction in PEM water electrolysers. J Power Sources 177:281–285. https://doi.org/10.1016/j.jpowsour.2007.11.072
8. Baglio V, Blasi DA, Denaro T, Antonucci V, Arico AS, Ornelas R (2008) Synthesis, characterization and evaluation of IrO$_2$-RuO$_2$ electrocatalytic powders for oxygen evolution reaction. J New Mater Electrochem Syst 11:105–108
9. Wang XX, Tan ZH, Zeng M, Wang JN (2014) Carbon nanocages: a new support material for Pt catalyst with remarkably high durability. Sci Rep 4:4437/1–4437/11. https://doi.org/10.1038/srep04437
10. Sheng Dang S, Gabriele C (2013) A perspective on carbon materials for future energy application. J Energy Chem 22:151–173. https://doi.org/10.1016/S2095-4956(13)60022-4
11. Pushkarev AS, Pushkareva IV, Grigoriev SA, Kalinichenko VN, Presniakov MY, Fateev VN (2015) Electrocatalytic layers modified by reduced graphene oxide for PEM fuel cells. Int J Hydrog Energy 40:14492–14497. https://doi.org/10.1016/j.ijhydene.2015.05.093
12. Naga Mahesh K, Sarada Prasad J, Venkateswer Rao M, Himabindu V, Yerramilli A, Rao R (2009) Performance of Pd on activated carbon as hydrogen electrode with respect to hydrogen yield in a single cell proton exchange membrane (PEM) water electrolyser.

Int J Hydrog Energy 34:6085–6088. https://doi.org/10.1016/j.ijhydene.2009.05.129

13. Ramakrishna SUB, Srinivasulu Reddy D, Shiva Kumar S, Himabindu V (2016) Nitrogen doped CNTs supported palladium electrocatalyst for hydrogen evolution reaction in PEM water electrolyser. Int J Hydrog Energy 41:20447–20454. https://doi.org/10.1016/j.ijhydene.2016.08.195

14. Nasini UB, Gopal Bairi V, Ramasahayam KS, Bourdo SE, Viswanathan T, Shaikh AU (2014) Oxygen reduction studies of phosphorus-nitrogen co-doped mesoporus carbon synthesized via microwave technique. Chem Electro Chem 1:573–579. https://doi.org/10.1002/celc.201300047

15. Yang D-S, Bhattacharjya D, Song MY, Yu J-S (2014) Highly efficient metal-free phosphorus-doped platelet ordered mesoporous carbon for electrocatalytic oxygen reduction. Carbon 67:736–743. https://doi.org/10.1016/j.carbon.2013.10.065

16. Zhang D, Han M, Lic YB, Leic L, Shangc Y, Wangc K, Wangc Y, Zhangc Z, Zhangc X, Feng H (2016) Phosphorus and sulfur dual doped hierarchic porous carbons with superior supercapacitance performance. Electrochim Acta 222:141–148. https://doi.org/10.1016/j.electacta.2016.10.184

17. Tharamani C, Nagaiah S, Kundu M, Bron M, Muhler M, Schuhmann W (2010) Nitrogen-doped carbon nanotubes as a cathode catalyst for the oxygen reduction reaction in alkaline medium. Electrochem Commun 12:338–341. https://doi.org/10.1016/j.elecom.2009.12.021

18. Mo Z, Zheng R, Peng H, Liang H, Liao S (2014) Nitrogen-doped graphene prepared by a transfer doping approach for the oxygen reduction reaction application. J Power Sources 245:801–807. https://doi.org/10.1016/j.jpowsour.2013.07.038

19. Imran Jafri R, Rajalakshmi N, Dhathathreyan KS, Ramaprabhu S (2015) Nitrogen doped graphene prepared by hydrothermal and thermal solid state methods as catalyst supports for fuel cell. Int J Hydrog Energy 40:4337–4348. https://doi.org/10.1016/j.ijhydene.2015.02.008

20. Jiao W, Yang Z, Li X, Sun Q, Jin C, Strasserd P, Yang R (2013) Phosphorus-doped porous carbons as efficient electrocatalysts for oxygen reduction. J Mater Chem A 1:9889–9896. https://doi.org/10.1039/C3TA11849E

21. Jo G, Shanmugam S (2012) Single-step synthetic approach for boron-doped carbons as a non-precious catalyst for oxygen reduction in alkaline medium. Electrochem Commun 25:101–104. https://doi.org/10.1016/j.elecom.2012.09.025

22. Yang L, Jiang S, Yu Z, Zhu L, Chen S, Wang X, Wu Q, Ma J, Ma Y, Hu Z (2011) Boron-doped carbon nanotubes as metal-free electrocatalysts for the oxygen reduction reaction. Angew Chem 123:7270–7273. https://doi.org/10.1002/anie.201101287

23. Choi CH, Park SH, Woo SI (2012) Phosphorus-nitrogen dual doped carbon as an effective catalyst for oxygen reduction reaction in acidic media: effects of the amount of P-doping on the physical and electrochemical properties of carbon. J Mater Chem 22:12107−12115. https://doi.org/10.1039/C2JM31079A

24. Choi CH, Park SH, Woo SI (2012) Binary and ternary doping of nitrogen, boron, and phosphorus into carbon for enhancing electrochemical oxygen reduction activity. ACS Nano 6:7084–7091. https://doi.org/10.1021/nn3021234

25. Nasini UB, Bairi VG, Ramasahayam SK, Bourdo SE, Viswanathan T, Shaikh AU (2014) Phosphorous and nitrogen dual heteroatom doped mesoporous carbon synthesized via microwave method for supercapacitor application. J Power Sources 250:257–265. https://doi.org/10.1016/j.jpowsour.2013.11.014

26. Wang C, Zhou Y, Sun L, Wan P, Zhang X, Qiu J (2013) Sustainable synthesis of phosphorus- and nitrogen-co-doped porous carbons with tunable surface properties for supercapacitors. J Power Sources 239:81–88. https://doi.org/10.1016/j.jpowsour.2013.03.126

27. Ma X, Ning G, Qi C, Xu C, Gao J (2014) Phosphorus and nitrogen dual-doped few-layered porous graphene: a high-performance anode material for lithium-ion batteries. ACS Appl Mater Interfaces 6:14415–14422. https://doi.org/10.1021/am503692g

28. Some S, Kim J, Lee K, Kulkarni A, Yoon Y, Lee S, Kim T, Lee H (2012) Highly air-stable phosphorus-doped n-type graphene field-effect transistors. Adv Mater 24:5481–5486. https://doi.org/10.1002/adma.201202255

29. Shiva Kumar S, Ramakrishna SUB, Rama Devi B, Himabindu V (2018) Phosphorus doped carbon nanoparticles supported palladium electrocatalyst for the hydrogen evolution reaction (HER) in PEM water electrolysis. Ionics 24:1–9. https://doi.org/10.1007/s11581-018-2471-0

30. Fırtına I, Guner S, Albostan A (2011) Preparation and characterization of membrane electrode assembly (MEA) for PEMFC. Int J Energy Res 35:146–152. https://doi.org/10.1002/er.1773

31. Millet P, Mbemba N, Grigoriev SA, Fateev VN, Aukauloo A, Etievant C (2011) Electrochemical performances of PEM water electrolysis cells and perspectives. Int J Hydrog Energy 36:4134–4142. https://doi.org/10.1016/j.ijhydene.2010.06.105

32. Ozcan A, Mohan K (2011) Equivalent electrical model for a proton exchange membrane (PEM) electrolyser. Energy Convers Manag 52:2952–2957. https://doi.org/10.1016/j.enconman.2011.04.007

33. Shiva Kumar S, Ramakrishna SUB, Rama Devi B, Himabindu V (2018) Phosphorus-doped graphene supported palladium (Pd/PG) electrocatalyst for the hydrogen evolution reaction in PEM water electrolysis. Int J Green Energy 15:1–10. https://doi.org/10.1080/15435075.2018.1508468

34. Yuan D, Xu C, Liu Y, Tan S, Wang X, Wei Z (2007) Synthesis of coin-like hollow carbon and performance as Pd catalyst support for methanol electro-oxidation. Electrochem Commun 9:2473–2478. https://doi.org/10.1016/j.elecom.2007.07.027

35. Ye F, Xu C, Liu G, Li J, Wang X, Xiaoze D, Lee JK (2018) A novel PtRuIr nanoclusters synthesized by selectively electrodepositing Ir on PtRu as highly active bifunctional electrocatalysts for oxygen evolution and reduction. Energy Convers Manag 155:182–187. https://doi.org/10.1016/j.enconman.2017.10.067

36. Millet P, Andolfatto F, Durand R (1996) Design and performance of a solid polymer electrolyte water electrolyser. Int J Hydrog Energy 21:87–93. https://doi.org/10.1016/0360-3199(95)00005-4

37. Grigoriev SA, Lyutikova E, Martemianov S, Fateev VN, Lebouin C, Millet P (2006) Palladium-based electrocatalysts for PEM applications. WHEC Lyon Fr 16:13–16

38. Martins CA, Fernandez PS, Lima F, Troiani HE, Martins ME, Arenillas A (2014) Remarkable electrochemical stability of one step synthesized Pd nanoparticles supported on graphene and multiwalled carbon nanotubes. Nano Energy 9:142–151. https://doi.org/10.1016/j.nanoen.2014.07.009

39. Shiva Kumar S, Ramakrishna SUB, Bhagawan D, Himabindu V (2017) Preparation of $Ru_xPd_{1-x}O_2$ electrocatalysts for the oxygen evolution reaction (OER) in PEM water electrolysis. Ionics 24:2411–2419. https://doi.org/10.1007/s11581-017-2359-4

40. Yang W, Chen B, Zhou C, Ma X, Hou L, Tang Y, Yang F, Ning G, Zhang L, Li Y (2017) Phosphorus-doped porous graphene nanosheet as metal-free electrocatalyst for triiodide reduction reaction in dye-sensitized solar cell. Appl Surf Sci 405:308–315. https://doi.org/10.1016/j.apsusc.2017.02.074

41. Abdin Z, Webb CJ, Gray EMA (2015) Modelling and simulation of a proton exchange membrane (PEM) electrolyser cell. Int J Hydrog Energy 40:13243–13257. https://doi.org/10.1016/j.ijhydene.2015.07.129

42. Shiva Kumar S, Ramakrishna SUB, Srinivasulu Reddy D, Bhagawan D, Himabindu V (2017) Synthesis of polysulfone and zirconium oxide coated asbestos composite separators for alkaline water electrolysis. Chem Eng Process Technol 3:1035/1–1035/6 ISSN: 2333-6633

43. Shiva Kumar S, Ramakrishna SUB, Vijaya Krishna S, Srilatha K, Rama Devi B, Himabindu V (2018) Synthesis of titanium (IV) oxide composite membrane for hydrogen production through alkaline water electrolysis. S Afr J Chem Eng 25:54–61. https://doi.org/10.1016/j.sajce.2017.12.004

44. Li K, Ling L, Lu C, Qiao W, Liu Z, Liu L (2001) Catalytic removal SO_2 over ammonia-activated carbon fibers. Carbon 39:1803–1808. https://doi.org/10.1016/S0008-6223(00)00320-1

45. Naga Mahesh K, Balaji R, Dhathathreyan KS (2016) Palladium nanoparticles as hydrogen evolution reaction (HER) electrocatalyst in electrochemical methanol reformer. Int J Hydrog Energy 41:46–51. https://doi.org/10.1016/j.ijhydene.2015.09.110